MedChemComm

Accepted Manuscript

This is an *Accepted Manuscript*, which has been through the Royal Society of Chemistry peer review process and has been accepted for publication.

Accepted Manuscripts are published online shortly after acceptance, before technical editing, formatting and proof reading. Using this free service, authors can make their results available to the community, in citable form, before we publish the edited article. We will replace this *Accepted Manuscript* with the edited and formatted *Advance Article* as soon as it is available.

You can find more information about *Accepted Manuscripts* in the Information for Authors.

Please note that technical editing may introduce minor changes to the text and/or graphics, which may alter content. The journal's standard Terms & Conditions and the Ethical guidelines still apply. In no event shall the Royal Society of Chemistry be held responsible for any errors or omissions in this *Accepted Manuscript* or any consequences arising from the use of any information it contains.

ROYAL SOCIETY OF CHEMISTRY

www.rsc.org/medchemcomm

MedChemComm

ARTICLE

Insight into the cytotoxicity, DNA binding and cell apoptosis induction of a zinc(II) complex of 5-bromo-8-hydroxylquinoline (HBrQ)

Received 00th January 20xx,
Accepted 00th January 20xx

DOI: 10.1039/x0xx00000x

www.rsc.org/

Hai-Rong Zhang[a,b,c], Yan-Cheng Liu[b*], Ting Meng[b], Qi-Pin Qin[b], Shang-Feng Tang[b], Zhen-Feng Chen[b], Bi-Qun Zou[b], You-Nian Liu[a] and Hong Liang[a,b*]

A new zinc(II) complex (**1**) with 5-bromo-8-hydroxylquinoline (HBrQ) was prepared and structurally characterized by ESI-MS, elemental analysis, ^{1}H and ^{13}C NMR, as well as single crystal X-ray diffraction analysis. The DNA binding study on complex **1** performed by UV-Vis, fluorescence and circular dichroism (CD) spectral analyses suggested that complex **1** interacted with ct-DNA mainly *via* an intercalative binding mode. The *in vitro* cytotoxicity of complex **1**, compared with $Zn(OAc)_2{\cdot}H_2O$, HBrQ and cisplatin, was screened against a series of tumor cell lines as well as the normal liver cell line HL 7702 by MTT assay. Complex **1** showed much higher cytotoxicity than $Zn(OAc)_2{\cdot}H_2O$ and HBrQ against most of the tumor cell lines, in which BEL-7404 was the most sensitive tumor cell line towards **1**, with IC_{50} value of 8.69 ± 0.04 μM. Complex **1** was found to greatly induce cell cycle arrest in the BEL-7404 cells at G2 phase, and consequently to induce the cell apoptosis in a dose-dependent mode suggested by the cell apoptosis analysis *via* Hoechst 33258 and AO/EB staining assays. Targeting the mitochondria pathway due to the redox activity of Zn, the apoptotic mechanism in the BEL-7404 cells treated by **1** was investigated by the reactive oxygen species (ROS) detection, intracellular calcium concentration measurement and caspase-9/3 activity assay, which showed that the cell apoptosis induced by **1** was closely related to the loss of mitochondrial membrane potential, ROS production and the enhancement of the intracellular $[Ca^{2+}]$, which would trigger the caspase-9/3 activation *via* a mitochondrial dysfunction pathway.

1. Introduction

In recent years, cancer has grown to be the second largest cause of death both in the developed world and China. It is of vital importance to discover and develop novel therapeutic anticancer agents, which has attracted considerable interests of many bioinorganic chemists.[1,2] Although cisplatin and the related Pt-based complexes have been used in clinic as effective anticancer drugs, their severe side effects, high toxicities and the acquired resistances still heavily restricted their clinical applications. During the past two decades, in the searching for new anticancer metallodrugs that can overcome the clinical drawbacks of routinely used Pt drugs, great efforts have been dedicated to the development of more effective and less toxic non-platinum metal-based drugs.[3-5]

Zinc is the second most prominent trace element in human body, which plays a very important role in human growth and development, reproductive and genetic, immune, endocrine and other important physiological process. Zinc can regulate the expression of many genes that are involved in antioxidant processes including metallothionein, glutamylcysteine synthetase and glutathione peroxidase, *via* the activation of the metal response transcription factor-1.[6] Zinc(II) is also regarded as a major regulatory ion in the metabolism of cells.[7] In addition, zinc possesses good coordination ability and low toxicity.[8] In recent twenty years, a series of zinc(II) complexes with anticancer activity have been reported, such as zinc(II) phthalocyanine tumor photosensitizers and zinc(II) complex bearing quinoline ligands.[9,10]

On the other hand, 8-hydroxyquinoline and its derivatives have attracted the medicinal chemists' great interests due to their significant pharmacological activities *in vitro* and *in vivo*, such as the antitumor activity.[11-13] A series of anticancer studies of 8-hydroxyquinoline have been reported. For example, Himmi et al. reported that 8-hydroxyquinoline's oxine processed antitumor and antimicrobial activities.[14] Chan et al. also found out that 8-hydroxyquinoline derivatives could be developed to effective antitumor agents.[15] Recently, 8-hydroxyquinoline derivative (clioquinol) entered the phase I clinical trials in patients with hematologic malignancy, including leukemia, myelodysplasia, non-Hodgkin's and Hodgkin's lymphomas, and multiple myeloma.[16]

[a] College of Chemistry and Chemical Engineering, Central South University, Changsha, Hunan, 410083, P.R. China.
[b] State Key Laboratory Cultivation Base for the Chemistry and Molecular Engineering of Medicinal Resources, School of Chemistry & Pharmaceutical Sciences, Guangxi Normal University, Guilin, Guangxi, 541004, P. R. China.
[c] Department of Chemistry and Material Science, Hunan University of Humanities, Science and Technology, Loudi, Hunan, 417000, PR China.
†*Corresponding authors: E-mail address: ycliugxnu@aliyun.com (Y. –C. Liu), hliang@gxnu.edu.cn (H. Liang) Address: No. 15 Yucai Road, Guilin, Guangxi 541004, China. Tel./Fax.: +86-773-2120958

Electronic Supplementary Information (ESI) available: The experimental section can be found in the supplementary materials (ESI). CCDC No. 1059676 for complex **1** contains the supplementary crystallographic data for this paper. The data can be obtained free of charge *via*http://www.ccdc.cam.ac.uk, or from the Cambridge Crystallographic Data Centre, 12 Union Road, Cambridge CB21EZ, UK (Fax: (+44) 1223-336-033; E-mail: deposit@ccdc.cam.ac.uk). See DOI: 10.1039/x0xx00000x

Since the 1960s, Gershon et al. explored hundreds of 5-/7-substituted 8-hydroxyquinoline derivatives in detail, especially on their Cu(II) complexes for the fungitoxicity.[17,18] It was found that the 5-/7-halo groups might enhance the antifungal activity of the 8-hydroxyquinoline. However, the antitumor activities of metal complexes of these 5-/7-halo-8-hydroxyquinoline derivatives were not fully explored, including the 5-bromo-8-hydroxylquinoline (HBrQ).[19] Since 2011, we have synthesized a series of metal complexes of 5,7-dihalo-8-hydroxyquinoline and screened their in vitro antitumor activities. The results also suggested the significance of the halogenated groups (F-, Cl-, I-) on enhancing the antitumor activities, in which some metal complexes of 5,7-dibromo-8-hydroxyquinoline showed much higher antitumor activities than the ligand.[20,21]

As a continuing work, a zinc(II) complex of 5-bromo-8-hydroxylquinoline (HBrQ) was synthesized and fully characterized in this study, which was primarily reported by Chou et al. in 1965.[22] With the research effort to explore new kind of potential antitumor agents, its DNA binding property was primarily studied and the *in vitro* cytotoxicity against a series of tumor cell lines was screened. Aiming to the most sensitive tumor cell line BEL-7404, the intracellular apoptotic pathway under the treatment of the zinc(II) complex was further studied and discussed for better understanding its possible antitumor mechanism.

2. Results and discussion

2.1 Structural characterization of complex 1

The X-ray diffraction analysis showed that complex **1** crystallized in a monoclinic system with space group $P2_1/c$. The crystal structure of complex **1** with labeled atoms was shown in Fig. 1. The details of crystallographic data and refinement parameters were listed in Table S1, and selected bond distances and angles for **1** were listed in Table S2. Complex **1** showed a simple mononuclear coordination structure in a centrosymmetric mode. The Zn(1) atom was six coordinated in an octahedral coordination geometry, in which two HBrQ ligands chelated to Zn(1) *via* the deprotonated hydroxyl O atom and the quinoline N atom to form the equatorial plane, while the two axial positions were occupied respectively by a methanol molecule. The bite angles of N(1)-Zn(1)-O(1) and N(1)-Zn(1)-O(2) were 80.02(14)° and 90.44(15)°, respectively (see Table S2). And no other solvent molecules were found in the crystal structure.

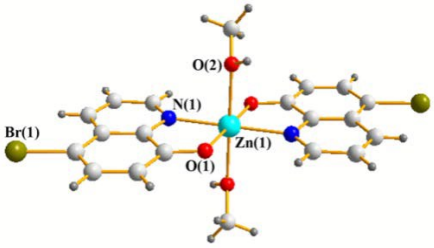

Fig. 1. The ball-stick presentation for the crystal structure of complex **1**.

Furthermore, the existing species of complex **1** in aqueous solution was studied by ESI-MS analysis, to analyze the exact species of the metal complex existing in solution state for better understanding its biological activity as well as the potential structure-activity relationship (SAR). As shown in Fig. S1, it was found that the maximum abundance of ESI-MS for **1** peaked at 546.7 in the negative ion mode, corresponding to $[Zn(BrQ)_2+H_2O+OH]^-$. It strongly suggested that complex **1** tended to maintain a mono-nuclear coordinating structure in aqueous solution, with a BrQ/Zn(II) ratio of 2:1. A weak peak at 699.1 in the negative ion mode was also found, which suggested the binuclear species, $[\mu_2\text{-}Zn_2(BrQ)_2+4H_2O+3OH]^-$ existed as a minor species of **1** in aqueous solution.

2.2 *In vitro* cytotoxicity screening by MTT assay

The cytotoxicities of complex **1** against five typical tumor cell lines (BEL-7404, HepG2, HeLa, T-24, MGC80-3), comparing with $Zn(OAc)_2{\cdot}H_2O$, HBrQ and cisplatin, were evaluated by MTT assay, and the human normal liver cell line HL-7702 was also tested for the selectivity study. The IC_{50} values of the tested compounds were listed in Table S3. The IC_{50} values of complex **1** were found to be much lower than those of HBrQ and $Zn(OAc)_2{\cdot}H_2O$, in which the BEL-7404 was the most sensitive cell line for **1** among these tested tumor cell lines, with the IC_{50} value of 8.69 ± 0.04 μM. It was at least 12 times of cytotoxicity than that of $Zn(OAc)_2{\cdot}H_2O$ or HBrQ (IC_{50} > 100 μM). Even compared with cisplatin (IC_{50} = 25.08 ± 0.12 μM), complex **1** also showed advantage on inhibiting the proliferation of the BEL-7404 cells, although the other tested tumor cell lines were not, as indicated in Fig. 2 and Table S3.

On the other hand, it should be noted that complex **1** also showed low cytotoxicity on the human normal liver cell line HL-7702, with the IC_{50} value of 28.40 ± 0.05 μM. In terms of the value, it was significantly higher than those for the tested tumor cell lines, especially for the BEL-7404 liver tumor cell line, which implied the better cytotoxic selectivity on the tumor cells of complex **1**.[24] The cytotoxicity of **1** against HL-7702 was also much lower than that of cisplatin (IC_{50} = 5.04 ± 0.06 μM), suggesting its potential for the better therapeutic effect on the liver cancer.

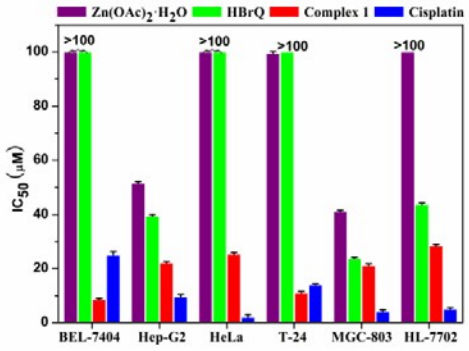

Fig. 2. IC_{50} (μM) values of complex **1**, comparing with $Zn(OAc)_2{\cdot}H_2O$, HBrQ and cisplatin, towards six typical human cell lines after incubation for 48 h.

2.3 DNA binding studies

The DNA replication in tumor cells can be blocked by the interactions between the small molecules and DNA. Since DNA is generally regarded as the primary antitumor target, it is necessary to study the DNA binding property of complex **1** for better understanding its antitumor activity. The DNA binding property of **1** was studied by UV-Vis, fluorescence and CD spectroscopic analyses.

2.3.1 UV-Vis spectral analysis

UV-Vis absorption spectroscopy is an effective method to examine the binding mode of small molecules with DNA. The electrostatic interaction of complex **1** with ct-DNA was primarily studied by UV-Vis absorption spectrum with increasing addition of SDS. Sodium dodecyl sulfonate (SDS) was an ideal probe to ascertain whether the electrostatic interaction existed due to the aggregated SDS anions acting as appropriate substitute for DNA polyanionic backbone, which led to spectral changes.[25] As indicated in Fig. S2, the addition of increasing amounts of SDS caused slight hypochromicity on the maximum absorbance of complex **1** at *ca.* 270 nm, which suggested a weak electrostatic interaction between **1** and DNA.

To ascertain the possible binding mode between complex **1** and DNA, the interaction of **1** with ct-DNA was also studied by UV-Vis spectral analysis. The absorption spectra of **1** in the absence and presence of ct-DNA were shown in Fig. 3. The maximum absorbance (A_{max} = 3.120) of **1** appeared at 265 nm in absence of ct-DNA, which could be attributed to the π–π^* electron transition of the aromatic structure of quinoline. After gradient addition of ct-DNA till the [DNA]/[**1**] ratio reached 7 : 1, the A_{max}(**1**) gradually red-shifted to 292 nm and gradually decreased to 0.999, with a total hypochromic ratio of 68% for **1**. It strongly suggested that complex **1** interacted with ct-DNA in an intercalative binding mode.[26,27]

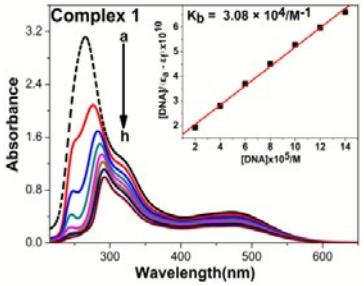

Fig. 3. The UV-Vis absorption spectra of complex **1** at 2.0 × 10^{-5} M in the absence (dashed line) and presence (solid lines) of increasing amounts of ct-DNA from 1 : 1 to 7 : 1.

To quantitatively elucidate the binding intensity of complex **1** with DNA, the intrinsic binding constant, K_b, was calculated using the following equation:[24,27]

$$\frac{[DNA]}{(\varepsilon_a-\varepsilon_f)}=\frac{[DNA]}{(\varepsilon_b-\varepsilon_f)}+\frac{1}{K_b(\varepsilon_b-\varepsilon_f)} \quad (1)$$

where [DNA] is the concentration of DNA in base pairs and ε_a is the observed extinction coefficient (A_{obsd}/[M]), ε_f and ε_b correspond to the extinction coefficient of the free compound and the extinction coefficient of the compound in the fully DNA-bound form, respectively. K_b is the intrinsic binding constant. The ratio of slope to intercept in the plot of [DNA]/(ε_a–ε_f) versus [DNA] gave the values of K_b, which was shown in the inset plot of Fig. 3. The intrinsic binding constant (K_b) of complex **1** with DNA was evaluated to be 3.08 × 10^4 M^{-1}, indicating a considerable intercalative binding intensity of **1** to DNA. Taking into account the ESI-MS analysis, it was believed that the coordination of BrQ to Zn(II) gave a more rigid structure of complex **1** than HBrQ, which facilitated the intercalative binding of **1** with DNA.

2.3.2 Fluorescence spectral analysis

The DNA binding property of complex **1** was also discussed by fluorescent spectral analysis, based on the competitive binding between EB and **1** with ct-DNA.[28,29] As shown in Fig. 4, the EB molecules bound by ct-DNA gave strong fluorescence emission with maximum emission intensity at 582 nm. Under the gradient addition of complex **1**, the fluorescent intensity of EB was gradually quenched. It indicated that there existed competitive binding between complex **1** and EB, which suggested an intercalative binding mode of **1** with DNA. The fluorescence quenching constant (K_q) was calculated according to Stern-Volmer equation:[30]

$$I_0 / I = 1 + K_q \times [Q] \quad (2)$$

where I_0 is the fluorescence intensity of EB bound by DNA in the absence of quencher, I is the fluorescence intensity EB in the presence of the quencher, complex **1**, and [Q] is the concentration of quencher. As indicated by the inset plot of Fig. 4, the fluorescence quenching constant (K_q) was calculated to be 2.07 × 10^4 M^{-1}, which suggested that the intercalative binding of complex **1** with ct-DNA was considerably strong which is consistent with the results of the above UV-Vis spectral analysis.

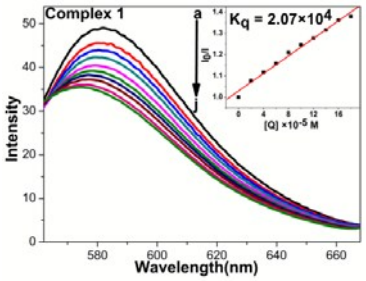

Fig. 4. Fluorescence spectra of EB bound by ct-DNA ([DNA] = 2.0 × 10^{-5}M, [EB] = 2.0 × 10^{-6}M) in the absence and presence of complex **1** with [**1**]/[EB] ratios range from 1:1 to 9:1.

2.3.3 CD spectral analysis

To further determine the intercalative binding of complex **1** with DNA, CD spectral titration analysis was also performed. As shown in Fig. 5, the CD spectra of ct-DNA alone showed the characteristic positive absorption band at 277 nm and the negative band at 244 nm, due to the base stacking and the helicity of B-type DNA, respectively.[31] As shown in Fig. 5, the

gradual addition of complex **1** induced significant decreases on both the positive and the negative CD absorption of ct-DNA. Since the groove binding and electrostatic interactions did not change the intensities of both the positive and negative CD spectra, and combining with the results from the above spectral analyses, the interaction between complex **1** and DNA should be confirmed as an intercalative binding mode.[25,27]

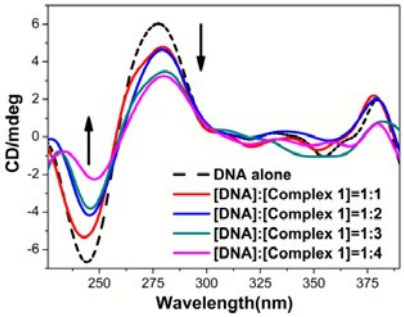

Fig. 5. CD spectra of ct-DNA (1.0×10^{-4} M) in the absence and presence of complex **1** with increasing concentrations ((1, 2, 3, 4) × 10^{-4} M) in Tris-HCl buffer at 25 °C (pH 7.4).

2.4 Cell cycle arrest

Since BEL-7404 was the most sensitive cell line towards complex **1** among the tested tumor cell lines, the cell cycle progression of the BEL-7404 cells treated by **1**, comparing with $Zn(OAc)_2{\cdot}H_2O$ and the free HBrQ, was primarily examined by using flow cytometric analysis, to explore the intracellular mechanism for its growth inhibition.

As shown in Fig. 6, the BEL-7404 cells treated by **1** for 48 h showed a dose-dependent accumulation in the G2 phase. With increasing concentrations of complex **1** from 0 to 4.5, 9.0, 18.0 μM, the G2 phase population increased from 3.16% (for control) till to 20.8%, while the population of S phase decreased from 39% (for control) to 30%. It suggested that complex **1** induced cell cycle arrest in BEL-7404 cells at G2 phase.[32] Since the G2/M cell cycle checkpoint is one of the crucial important responses to the DNA damage, it further suggested that DNA was an important intracellular target for complex **1**. In contrast, only the HBrQ or $Zn(OAc)_2{\cdot}H_2O$ alone showed no significant effect on arresting the cell cycle at G2 phase in BEL-7404 cells in the concentration range from 4.5, 9.0 till to 18.0 μM.

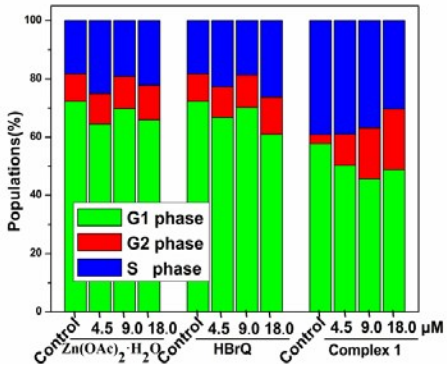

Fig. 6. The percentage of cell populations in various phases (G1, S and G2 phase) for the cell cycle distribution in BEL-7404 cells treated by 4.5, 9.0, 18.0 μM of complex **1**, HBrQ and $Zn(OAc)_2{\cdot}H_2O$, for 48 h.

2.5 Cell apoptosis assay

The cell cycle arrest was considered to play an essential role in tumor cells apoptosis, and the apoptosis induction was regarded as an antitumor approach for many bioactive agents.[33,34] To detect whether the growth inhibition on BEL-7404 cells was due to the cell apoptosis induced by **1**, the cell apoptosis assay was tested by flow cytometry, $Zn(OAc)_2{\cdot}H_2O$ and the free HBrQ was also set for comparison. The cells were double stained by Annexin V–FITC (to detect the characteristic phosphatidylserine residues in the early stage of apoptosis translocated from the inner cell membrane to outside) and PI (to examine the membrane permeation in necrotic cells).

It was found that the BEL-7404 cells treated by $Zn(OAc)_2{\cdot}H_2O$ or HBrQ alone at the maximum concentration of 18.0 μM did not show obvious accumulations on both the early stage and the late stage, as shown in Fig. 7. However, the BEL-7404 tumor cells incubated with complex **1** of gradient concentrations (0, 4.5, 9.0, 18.0 μM) for 8 h led to continuous increment on the percentage of the apoptotic cells in late stage, from 3.1% to 2.3, 32.2 and 37.6%, respectively (see Q2 zone). Moreover, the percentage of the early stage apoptotic cells also increased from 1.0% to 3.9, 18.9 and 22.4%, respectively (see Q3 zone). The significant increments on the apoptotic tumor cells both in the late stage and early stage strongly suggested that complex **1** could effectively induce the apoptosis in the BEL-7404 cells in a dose-dependent mode.

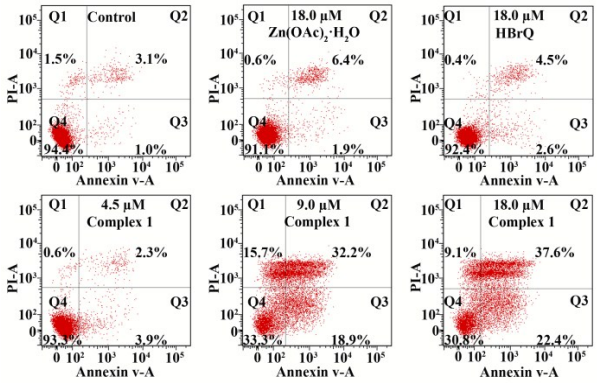

Fig. 7. The cell apoptosis induction in the BEL-7404 cells treated by complex **1** (4.5, 9.0, 18.0 μM), HBrQ (18.0 μM) and $Zn(OAc)_2{\cdot}H_2O$ (18.0 μM) for 8 h was examined by flow cytometry using PI and Annexin V-FITC double staining assay.

2.6 Morphological characterization of cell apoptosis by Hoechst 33258 and AO/EB staining

The morphological changes (cell shrinkage, chromatin condensation, nuclear fragmentation, formation of apoptotic

bodies) may be observed during the cell apoptosis process.[35] To further confirm the cell apoptosis induced by complex **1**, morphological changes in the BEL-7404 cells were observed under the fluorescent microscope by using the Hoechst 33258 staining and AO/EB double staining, respectively.

As shown in Fig. 8A, after treated with complex **1** of gradient concentrations (4.5, 9.0, 18.0 μM) for 8h, more and more tumor cells with apoptotic features (cell shrinkage and nucleus fragmentation) could be observed, comparing with the living cells for control. While as shown in Fig. 8B, after the tumor cells were treated by complex **1** with the increasing concentrations and double stained by AO/EB, more and more tumor cells showed typical apoptotic features, such as the formation of apoptotic bodies. Comparing with the living cells who emitted the green fluorescence, the apoptotic cells could be recognized under the fluorescent microscope, such as the bright green or orange fluorescence observed in the nuclear chromatin of the early-stage apoptotic cells, and the orange-red fluorescence observed in the nuclear chromatin of the late-stage apoptotic cells.[36]

Thus, viewed from the characteristic cellular morphology in the stained BEL-7404 cells, complex **1** could effectively induce cell apoptosis in the BEL-7404 tumor cells in a concentration-dependent manner. In contrast, the incubation with only the $Zn(OAc)_2{\cdot}H_2O$ or HBrQ at the maximal concentrations (18.0 μM) showed no obvious apoptotic features in the stained BEL-7404 cells. This is in agreement with their poor growth inhibitions and cell apoptosis inductions on the tested tumor cells, which clearly indicated that it was the complex **1** in coordinated state who exerted the significant antitumor activity, but not the zinc(II) or HBrQ alone. This has been also indicated by the recent study of Ikeda et al. on the zinc complex of Rutin, which suggested that the increase in biological activity of Rutin-Zn(II) complex could be associated with the coordination of Zn(II).[8]

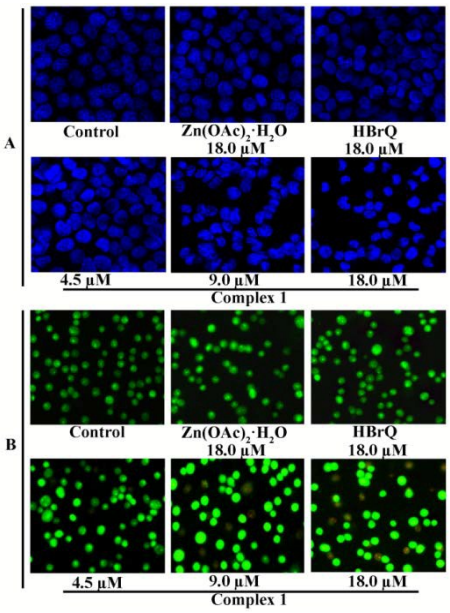

Fig. 8. Morphological observation on the apoptosis of the BEL-7404 cells stained by Hoechst 33258 staining (A) and AO/EB staining (B), when incubated with complex **1** (4.5, 9.0, 18.0 μM) or 18.0 μM of HBrQ or $Zn(OAc)_2{\cdot}H_2O$ for 8 h, respectively.

2.7 The mitochondria-mediated pathway assay for cell apoptosis

Mitochondrion is a vital cell organ which controls the cell apoptosis by regulating the mitochondrial membrane potential ($\Delta\psi$). The loss of $\Delta\psi$ is regarded as a key factor to detect the cell apoptosis in the early stage.[37] To further determine the cell apoptosis induced by complex**1**, the intracellular $\Delta\psi$ in the BEL-7404 cells was examined by flow cytometry, in which Rh123 was used as the staining probe molecules. As indicated in Fig. 9(a), the right marker was considered as the mitochondria with higher membrane potential, i.e. polarized mitochondria, and the left marker was regarded as the mitochondria with lower membrane potential, i.e. depolarized mitochondria. Comparing with the control, the polarization ratio of the mitochondria in the tumor cells treated by 9.0 μM of **1** decreased from 51.1% to 43.8%, suggesting that the cell apoptosis in the BEL-7404 cells induced by **1** might be an intrinsic mitochondria-mediated pathway.[38]

In the apoptotic cells, the over-expression of intracellular reactive oxygen species (ROS), which consists of some radical species and non-radicals hydrogen peroxide, is an important factor to cause damage on DNA and proteins, and plays a key role in the metabolism, oxidative stress, signal transduction and cell apoptosis. ROS generation is thought to directly activate the mitochondrial permeability transition and results in the loss of mitochondrial membrane potential and the membrane integrity.[39] Whether the ROS generation could be induced in BEL-7404 cells by complex **1** was thus further examined by flow cytometry using the DCFH-DA staining, since DCFH-DA can change to the fluorescent DCF when bound with ROS. As indicated in Fig. 9(b), compared with the control, the level of ROS generation in the tumor cells significantly enhanced from 50.0% to 64.1% under the treatment of 9.0 μM of complex **1** for 8 h. So the cell apoptosis induced by complex **1** was suggested to be closely related to the ROS-mediated mitochondrial dysfunction pathway, especially in the early-stage apoptosis.

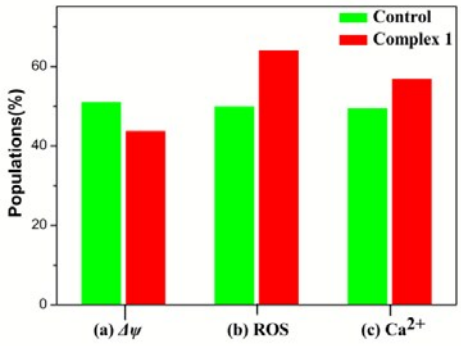

Fig. 9. (a) The BEL-7404 cells treated with 9.0 μM of complex **1** for 8 h and stained by Rh123 indicated the loss of the mitochondrial membrane potential ($\Delta\psi$) by flow cytometry. **(b)** The increment on the ROS generation in the BEL-7404 cells

when treated with 9.0 μM of complex **1** for 8 h.**(c)**The detection on the intracellular level of $[Ca^{2+}]_c$in the BEL-7404 cells treated with 9.0 μM of complex **1** for 8 h by flow cytometry using Fluo-3/AM as the fluorescent probe.

And considering the close relationship between the ROS generation and the released $[Ca^{2+}]$ in the intracellular level,[40] as well as the enhanced intracellular $[Ca^{2+}]$ being regarded as one of the major contributing factors towards the cell apoptosis by regulating the enzyme activity and disrupting the mitochondrial function,[41] the intracellular $[Ca^{2+}]$ of the BEL-7404 cells treated with complex **1** was further evaluated by flow cytometry using the fluorescent probe, Fluo-3/AM. As shown in Fig. 9(c), the $[Ca^{2+}]_c$ in the BEL-7404 cells indicated by Fluo-3/AM enhanced from 49.6% (for control) to 56.9% (in the presence of **1** at 9.0 μM). Combined with the above results, it clearly showed the ROS generation as a precursor to enhanced the intracellular $[Ca^{2+}]_c$ levels. These results proposed the mitochondrial apoptotic pathway induced by **1** *via* the mitochondria dysfunction triggered by ROS generation, which could be proven by the enhancement of the intracellular $[Ca^{2+}]_c$ levels.

2.8 Assessment on the Caspase-9/3 activation for cell apoptosis

The loss of mitochondrial membrane potential is regarded as an intracellular event, which will lead to the release of cytochrome C from mitochondria into the cytosol and subsequently activate caspase-9 and caspase-3.[42,43] Caspase-9 and caspase-3 play the essential roles as an initiator and an executor, respectively, in the cell apoptosis. To further confirm the intrinsic mitochondrion-mediated apoptotic pathway induced by complex **1**, the activation of caspase-9 and caspase-3 in the BEL-7404 cells was assessed by flow cytometry using FITC-DEVD-FMK (for caspase-3) and FITC-LEHD-FMK (for caspase-9) as probe molecules, respectively. As shown in Fig. 10, comparing with the control, the caspase-9 was found to be remarkably activated in the tumor cells treated with 9.0 μM of complex **1**, with activity ratios increasing from 3.2% to 55.6%. Subsequently, the caspase-3 was also activated by **1**, with activity ratios increasing from 0.7% (for control) to 31.6% (in the presence of 1 at 9.0 μM). It strongly suggested that complex **1** could effectively trigger the activation of caspase-9 as the initiator of the caspase cascade, and then activate the caspase-3 as the downstream protein of the caspase cascade.

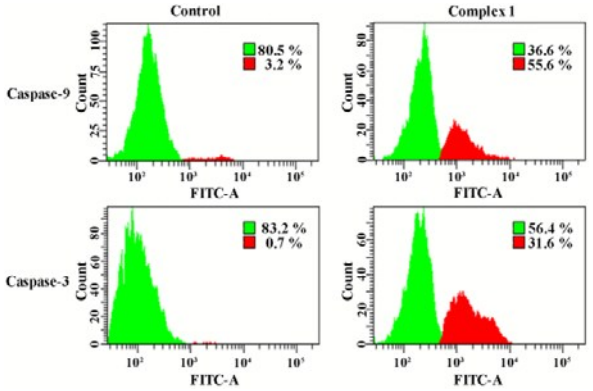

Fig. 10. The activation of caspase-9/3 in the BEL-7404 cells when treated with 9.0 μM of complex **1** for 8 h.

All these results above fully demonstrated that the cell apoptosis induced by **1** undergo the mitochondrion-mediated apoptotic pathway by activating the caspase cascade based on the ROS generation and intracellular release of $[Ca^{2+}]_c$ although other possible pathways should not be excluded. This significant apoptotic property of complex **1** were also found in some other zinc(II) complexes bearing different bioactive ligands, as recently reported.[44-46] For example, Pucci et al. reported a series of zinc(II) complexes of curcumin, which showed similar effective apoptotic induction on the tumor cell line SH-SY5Y in a dose-dependent mode too, involved the activation of JNK, caspase-3 and changes in MMP.[44] Liao et al. reported a zinc complex of a novel polysaccharide, DPI, which showed much more similar apoptotic mechanism to that of complex **1**, including the activation of caspase cascade, mitochondrial dysfunction and ROS overproduction. Intriguingly, the DPI-Zn complex led to the S phase cell cycle arrest in the MCF-7 tumor cells, which was different to that of **1**.[45] This may be also due to the different action mechanism of the corresponding ligands.[46]

3. Conclusions

In this paper, a new zinc(II) complex of 5-bromo-8-hydroxylquinoline (HBrQ) was synthesized and fully characterized. This complex formed as a mono-nuclear zinc(II) complex both in the crystallized state and in the aqueous solution state, implying the stability of this complex to maintain the coordinated state of BrQ to Zn(II). This complex most probably bound with DNA *via* an intercalative binding mode, and it was more cytotoxic to a series of typical human tumor cell lines than HBrQ, in which the BEL-7404 cell line was the most sensitive one. Its antitumor mechanism was studied on the cellular level targeting the mitochondrial pathway for cell apoptosis, due to the detected ROS generation and the intracellular Ca^{2+} release. From this study, it strongly suggested that the presence of this complex in the BEL-7404 cells induced the mitochondria-mediated apoptotic pathway by activating the caspase cascade. In this pathway, the ROS generation and the enhancement of intracellular $[Ca^{2+}]_c$ level were obviously observed, which was closely related to the mitochondria dysfunction.

Similar to our previous studies, HBrQ or the zinc(II) alone would not significantly induce cell apoptosis in the tested tumor cells. So it implied that the cell apoptosis induced by this complex could be ascribed to the coordination mode of BrQ to Zn(II), in which the rigid planar structure and the positive-charged Zn(II) as the metal centre should play the key roles for better DNA targeting property and the ROS generation in mitochondrion. This has also been proposed by some other recent studies. A study on the Cu(II)/Zn(II) complex of oxindolimine by Miguel et al indicated that the more rigid conformation of the metal complex facilitated its interaction with the intracellular target, CDK1/cycline B protein.[46] The recent study on the Zn(II) complex of Rutin by Ikeda et al also supported that the coordination of Zn(II) to the ligand was crucial to achieve better antitumor activity.[8] Nevertheless, the network of the apoptotic pathway in tumor cells is so complicated that other possible apoptotic pathways attributed to this complex may not be excluded. For example, the presence of this complex in the tested tumor cells enhanced the ROS release and intracellular $[Ca^{2+}]_c$, from *ca.* 50% to 64% and 57%, respectively. But these enhancement ratios were not so proportionate to those for the activation of caspase-9/3, which showed significant enhancements from *ca.* 3.3% to 55% and 0.7 to 32%, respectively. It might imply that other pathways also existed to activate the caspase cascade under the interaction of this Zn(II) complex, which need to be further studied for better understandings.[44,47]

Acknowledgements

This work was financially supported by the National Basic Research Program of China (Nos. 21271051, 81473102), and the Natural Science Foundation of Guangxi Province (No. 2013GXNSFAA019044).

Notes and references

1 Y. W. Jung and S. J. Lippard, *Chem. Rev.*, 2007, **107**, 1387–1407.
2 X. Wang and Z. Guo, *Chem. Soc. Rev.*, 2013, **42**, 202–224.
3 A. L. Noffke, A. Habtemariam, A. M. Pizarro and P. J. Sadler, *Chem. Commun.*, 2012, **48**, 5219–5246.
4 V. S. Stafford, K. Suntharalingam, A. Shivalingam, A. J. P. White, D. J. Mann and R. Vilar, *Dalton Trans.*, 2015, **44**, 3686–3700.
5 M. A. Jakupec, M. Galanski, V. B. Arion, C. G. Hartinger and B. K. Keppler, *Dalton Trans.*, 2008, 183–194.
6 J.-J. Zheng, Y. Zhang, W.-T Xu, Y.-B. Luo, J.-R. Hao, X.-L. Shen, X. Yang, X.-H. Li and K.-L. Huang, *Toxicol. Appl. Pharmacol.*, 2013, **268**, 123–131.
7 T. P. Stanojkovic, D. Kovala-Demertzi, A. Primikyri, I. Garcia-Santos, A. Castineiras, Z. Juranic and M. A. Demertzis, *J. Inorg. Biochem.*, 2010, **104**, 467–476.
8 N. E. A. Ikeda, E. M. Novak, D. A. Maria, A. S. Velosa and R. M. S. Pereira, *Chem-Biol. Interact.*, 2015, **239**, 184–191.
9 E. A. Enyedy, N. V. Nagy, E. Zsigo, C. R. Kowol, V. B. Arion and B. K. Keppler, T. Kiss, *Eur. J. Inorg. Chem.*, 2010, 1717–1728.
10 J. Lu, J.-L. Li, Q. Sun, L. Jiang, W. Gu, X. Liu, J.-L. Tian and S.-P. Yan, *Spectrochimica Acta, Part A*, 2014, **130**, 1386–1425.
11 Y. Song, H. Xu, W. Chen, P. Zhan and X. Liu, *Med. Chem. Commun.*, 2015, **6**, 61–74.
12 S. Zhai, L. Yang, Q. C. Cui, Y. Sun, Q. P. Dou and B. Yan, *J. Biol. Inorg. Chem.*, 2010, **15**, 259–269
13 É. A. Enyedy, O. Dömötör, K. Bali, A. Hetényi, T. Tuccinardi and B. K. Keppler, *J. Biol. Inorg. Chem.*, 2015, **20**, 77–88.
14 B. M. B. Himmi, S. Kitane, A. Eddaif, A. Alaoui, A. Bouklou and M. Soufiaoui, *Hydrometallurgy*, 2008, **93**, 39–44.
15 S.-H. Chan, C.-H. Chui, S.-W. Chan, S. H. L. Kok, D. Chan, M. Y. T. Tsoi, P. H. M. Leung, A. K. Y. Lam, A. S. C. Chan, K. H. Lam and J. C. O. Tang, *ACS Med. Chem. Lett.*, 2013, **4**, 170–174.
16 V. Oliveri, M. Viale, G. Caron, C. Aiello, R. Gangemi and G. Vecchio, *Dalton Trans.*, 2013, **42**, 2023–2034.
17 H. Gershon, *J. Med. Chem.*, 1974, **17**(8), 824–827.
18 H. Gershon, M. Gershon and D. D. Clarke, *Curr. Trends Med. Chem.*, 2006, **4**, 27–32.
19 P. Vranec, I. Potočňák, D. Sabolová, V. Farkasová, Z. Ipóthová, J. Pisarčíková and H. Paulíková, *J. Inorg. Biochem.*, 2014, **13**, 37-46.
20 Z.-F. Chen, X.-Y. Song, Y. Peng, X. Hong, Y.-C. Liu and H. Liang, *Dalton Trans.*, 2011, **40**, 1684–1692.
21 Y.-C. Liu, J.-H. Wei, Z.-F. Chen, M. Liu, Y.-Q. Gu, K.-B. Huang, Z.-Q. Li and H. Liang, *Eur. J. Med. Chem.*, 2013, **69**, 554–563.
22 (a) F.-C. Chou, Q. Fernando and H. Freiser, *Anal. Chem.*, 1965, **37**(3), 361–363; (b) F.-C Chou and H. Freiser, *Anal. Chem.*, 1968, **40**(1), 34–39.
23 H. Gershon and D. D. Clarke, *Monatshe für Chemie* (*Chemical Monthly*), 1991, **122**, 935–941.
24 A. Haleel, P. Arthi, N. D. Reddy, V. Veena, N. Sakthivel, Y. Arun, P. T. Perumal and A. K. Rahiman, *RSC Adv.*, 2014, **4**, 60816–60830.
25 D.-L. Ma and C.-M. Che, *Chem. Eur. J.*, 2003, **9**, 6133–6144.
26 H.-K. Liu and P. J. Sadler, *Acc. Chem. Res.*, 2011, **44**(5), 349-359.
27 V. M. Manikandamathavan, T. Weyhermüller, R. P. Parameswari, M. Sathishkumar, V. Subramanian and B. U. Nair, *Dalton Trans.*, 2014, **43**, 13018–13031.
28 P. Li, M.-J. Niu, M. Hong, S. Cheng and J.-M. Dou, *J. Inorg. Biochem.*, 2014, **137**, 101–108.
29 J.-H. Wen, C.-Y. Li, Z.-R. Geng, X.-Y. Ma and Z.-L. Wang, *Chem. Commun.*, 2011, **47**, 11330–11332.
30 J. R. Lakowicz and G. Weber, *Biochemistry*, 1973, **12**, 4161-4170.
31 A. D. Richards and A. Rodger, *Chem. Soc. Rev.*, 2007, **36**, 471-483.
32 S. Arora and S. Tandon, *Homeopathy*, 2015, **104**, 36–47.
33 L. Fan, Y.-L. Ma, Y. Liu, D.-P. Zheng and G.-G. Huang, *Eur. J. Pharmacol.*, 2014, **743**, 79–88.
34 G. Alexandre, H. Philippe, T. Marion, M. Patrice, C. M. Carole and V. Céline, *Int. J. Pharm.*, 2015, **479**, 422–429.
35 B. Saha, A. Mukherjee, S. Samanta, S. Paul, D. Bhattacharya, C. R. Santra and P. Karmakar, *Med. Chem. Commun.*, 2012, **3**, 1393–1405.
36 H.-L. Huang, Z.-Z. Li, Z.-H. Liang, J.-H. Yao and Y.-J. Liu, *Eur. J. Med. Chem.*, 2011, **46**, 3282–3290.
37 D. R. Green, *Cell*, 1998, **94**, 695–698.
38 N. Zamzami, C. Maisse, D. Metivier and G. Kroemer, *Methods Cell Biol.*, 2007, **80**, 327–340.
39 W.-D. Ma, Y.-P. Zou, P. Wang, X.-H. Yao, Y. Sun, M.-H. Duan, Y.-J. Fu and B. Yu, *Food Chem. Toxicol.*, 2014, **70**, 1–8.
40 V. Pachauri, A. Mehta, D. Mishra and S. J. S. Flora, *NeuroToxicology*, 2013, **35**, 137–145.
41 Z.-Y Xie, Y.-M. Zhang, A.-L. Li, P. Li, W.-H. Ji and D.-J. Huang, *Toxicol. Lett.*, 2010, **192**, 115–118.
42 W. C. Earnshaw, L. M. Martins and S. H. Kaufmann, *Annu. Rev. Biochem.*, 1999, **68**, 383–424.
43 R. U. Janicke, M. L. Sprengart, M. R. Wati and A. G. Porter, *J. Biol. Chem.*, 1998, **273**, 9357–9360.

44 D. Pucci, A. Crispini, B. S. Mendiguchía, S. Pirillo, M. Ghedini, S. Morelli and L. De Bartolo, *Dalton Trans.*, 2013, **42**, 9679–9687.
45 W. Liao, Y. Lu, J. Fu, Z. Ning, J. Yang and J. Ren, *J. Agric. Food Chem.*, 2015, **63**, 6525–6534.
46 R. B. Miguel, P. A. D. Petersen, F. A. Gonzales-Zubiate, C. C. Oliveira, N. Kumar, R. R. do Nascimento, H. M. Petrilli and A. M. da Costa Ferreira, *J. Biol. Inorg. Chem.*, 2015, **20**, 1205–1217.
47 T. Srdić-Rajić, M. Zec, T. Todorović, K. Anđelković and S. Radulović, *Eur. J. Med. Chem.*, 2011, **46**, 3734–3747.